Electrical Engineering (2022) 104:4137–4147
https://doi.org/10.1007/s00202-022-01612-6

ORIGINAL PAPER

The effect of water on tracking failure of epoxy/MgO samples

Kaancan Kirkagac[1] · Mehmet Murat Ispirli[2] · Aysel Ersoy[1]

Received: 25 March 2021 / Accepted: 29 June 2022 / Published online: 3 August 2022

Abstract
In this study, the change in the electrical performance of epoxy/MgO, which is one of the materials used to increase the performance of epoxy resin, was evaluated under the effect of water. Accordingly, comparative tracking index (CTI) experiments, which are one of the effective methods used to model electricity's effect on surface properties, were used. To measure the performance of epoxy resins without additions, 1%, 3% and 5% nanosized MgO-added samples were prepared. Prepared samples were stored 24 h, 48 h, 72 h, 96 h and 120 h in pure water. Then, the samples were subjected to CTI test in a laboratory environment. Recorded leakage current from experiments was analyzed using harmonic analysis. While the experimental results obtained have resulted in improvements like those of MgO/epoxy additions previously reported in the literature, the resistance of the observed samples after their exposure to pure water has been reported, in the opposite direction. Thus, with this experimental study, it has been demonstrated that it is necessary to add some hydrophobic compounds to show the desired performance in the external environment with MgO-doped epoxy resins. It should be supported by extra protection in such dense liquid environments.

Keywords Tracking failure · Epoxy resin · Harmonic distortion · Comparative tracking index

1 Introduction

Epoxy resin has become an important insulation material for electrical and electronic devices due to its excellent mechanical and electrical performance. Its physical and chemical properties play a vital role in the dielectric performance and reliability of most electrical systems [1, 2]. Nanocomposite materials are hybrid materials with a size of 1 to 100 nm. Polymer nanocomposites have many advantages despite pure filling polymer. Thanks to the addition, a polymer can be improved its electrical, mechanical and thermal properties, such as electrical conductivity, dielectric strength, capacitance, dielectric constant, tensile strength and elasticity. Thus, the safety and reliability of insulation materials can be increased, and costs of system integration and maintenance can be decreased [3–5].

There are some studies for improving the tracking performance of epoxy resin by adding different materials to epoxy samples in the literature. In [6–9], epoxy/MgO composite samples were prepared by adding 0.1%, 1%, 2%, 6% and 10% MgO to the epoxy resin and tracking tests were carried out on the surface. They observed that the tracking failure decreased due to increased MgO concentration by weight in these studies. In [10], epoxy/TiO_2 composite samples were prepared by adding 1%, 3%, 5% and 7% TiO_2 to the epoxy resin. As a result of DC tracking tests in these samples, while the tracking formation behavior and erosion gradually decreased in samples with 0–5% concentration, the opposite results were observed in samples with a concentration of 5–7%. Epoxy samples were prepared by adding 50% SiO_2, and in these studies, thermal properties and stability of epoxy composite samples were investigated [11, 12]. The thermal conductivity of epoxy resin is lower than metal and ceramic, and it is preferred as a coating material in the electrical and electronic industry. Tracking tests of nanoclay-added epoxy samples were carried out, and it is found that the amplitude of leakage current decreased with increased nanoclay rate in epoxy resin [13, 14]. Epoxy/Al_2O_3 were prepared by adding

✉ Kaancan Kirkagac
kaancan.kirkagac@gmail.com

Mehmet Murat Ispirli
mispirli@marmara.edu.tr

Aysel Ersoy
aersoy@iuc.edu.tr

[1] Department of Electrical - Electronics Engineering, Istanbul University-Cerrahpasa, Istanbul 34320, Turkey

[2] Department of Electrical - Electronics Engineering, Marmara University, Istanbul 34722, Turkey

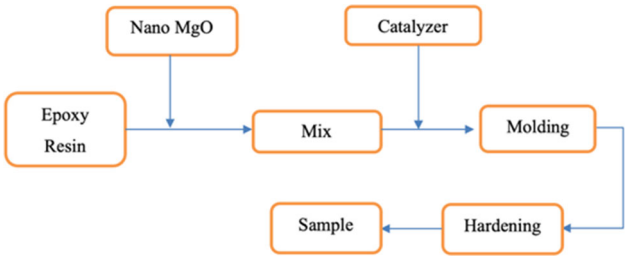

Fig. 1 Block diagram of sample preparation steps

different rates, and they were tested in terms of electrical properties [15–18]. The tracking resistance also increased with the addition of Al_2O_3. Thus, dielectric losses in epoxy resin decreased. The prepared epoxy resin was stored in pure water for 24 h, 48 h, 72 h, 96 h and 120 h to determine the resistance of epoxy resin against heat, water absorption and their multiple effects [19]. The tracking resistance of epoxy resin significantly decreased with increased water absorption time.

Nano-MgO has an excellent electrical insulating property. Nano-MgO is used in the radio industry for high-precision magnetic rod antenna, insulating material filling and magnetic material filling. In this paper, in order to investigate the effect of nano-MgO on tracking resistance, epoxy/MgO composite samples were prepared by adding 1%, 3% and 5% MgO to the epoxy resin. Some of the prepared samples were stored in pure water for 24 h, 48 h, 72 h, 96 h and 120 h. Another part of the prepared samples did not apply any aging process. Then, these aged and non-aged samples were tested by the comparative tracking index test method. Leakage currents were recorded from the surface of the sample during these experiments. Leakage currents were analyzed by the harmonic analysis method using Fourier transform. As a result, these experiments were evaluated in terms of weight loss of samples, droplet number of the beginning of carbonization, droplet number of the beginning of cavitation and harmonic orders.

2 Materials and methods

2.1 The preparation of test samples

The epoxy resin used in samples is a two-component, reaction-drying epoxy resin. In the preparation of the samples, the weight ratio of mixed is 1.6:1 (epoxy: hardener). These are catalyzer (hardener) and epoxy resin, respectively. In this study, commercially available Nanografi Nano Technology product with 98% purity, 20 nm MgO was used to prepare epoxy/MgO composites. Preparation steps of samples are shown in Fig. 1. First, nanosized MgO particles were added to the pure epoxy resin mixture. 1%, 3% and 5% by

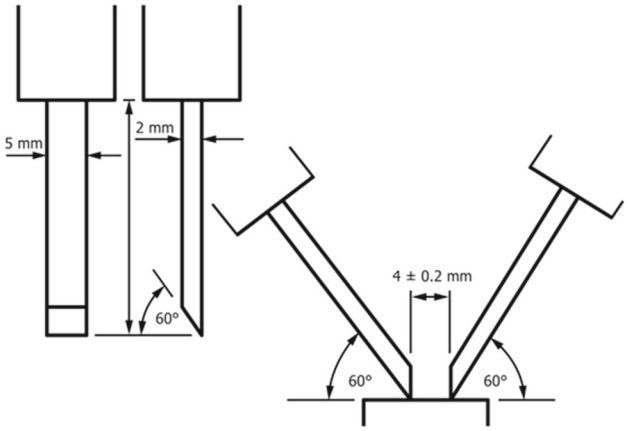

Fig. 2 Electrode arrangement used in the test setup [31]

weight of nano-MgO particles, respectively, were added to the mixing bowl before catalyzer was added. Then, these mixtures were mixed homogeneously and catalyzer (hardener) was added. In this way, homogeneous epoxy/MgO composites have been obtained. The prepared mixtures were molded in the size 12 cm × 5 cm × 0.5 cm. The surfaces of the samples that were kept in molds for 18 h were evaluated by visual inspection after they hardened.

These samples prepared in a laboratory environment were kept in pure water for 24 h, 48 h, 72 h, 96 h and 120 h in order to observe the aging effect of water which is one of the environmental factors. The aging container is an airtight glass container with a depth of 10 cm and dimensions of 30 × 40 cm. The temperature of the water in the aging container was 20 °C.

2.2 The experimental setup

ASTM-D5288 and IEC 60,112 test standard is used to evaluate the tracking resistance performance of insulation materials from low voltages up to 600 V [20]. The main purpose of this method is to evaluate the comparative tracking resistance performance under wet and dirty conditions. Firstly, IEC 60,112 was published in 1959 and then has been revised many times. In this study, the test setup was prepared based on ASTM D5288-14, which was the revised last version in 2014 [21]. Electrolyte drops are dropped on the sample surface at 30 ± 5 s intervals during the experiment. At the end of 50 drops, the experiment is finished. Experiments were repeated 5 times for every condition as indicated in the relevant standard. The electrolyte is a solution approximate concentration of 0.1% NH_4CI. According to ASTM D5288-14 standard, the resistivity of the test solution must be 385 ± 5 Ω cm at 23 ± 0.5 °C ambient temperature [21]. The electrode arrangement in the test setup is shown in Fig. 2. The width of copper electrode in the test setup is 5 mm and its thickness is 2 mm. It is placed symmetrically on the sample so

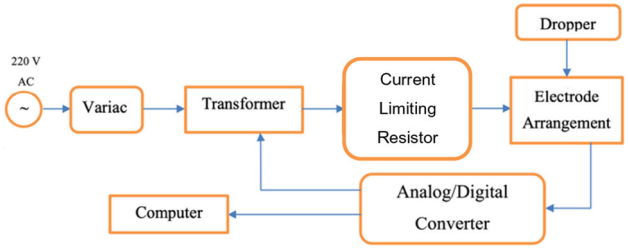

Fig. 3 Block diagram of the experimental setup

that the angle between the electrodes is $60 \pm 5°$ [20, 21]. The distance between the electrodes should be 4 ± 0.2 mm. Tests must be carried out at 20 ± 5 °C ambient temperature and in a draft-free environment. The current between the electrodes should not exceed 0.5 A for 2 s during the experiments. The block diagram of the used experimental setup is shown in Fig. 3. Here, variac is used to arrange the applied voltage. The leakage current was recorded in the experimental setup by A/D converter, which sample rate is 48 kHz. The top photograph of the experimental setup and the side photograph of electrode arrangement are shown in Fig. 4. In this study, 1%, 3% and 5% nanosized MgO-added samples were prepared. Later, these prepared samples were kept in pure water for 24 h, 48 h, 72 h, 96 h and 120 h. Finally, the samples were subjected to CTI test in a laboratory environment under 400 V, 500 V and 600 V [22].

2.3 The harmonic analysis of leakage current

Harmonic components are frequently used when investigating the deterioration of polymeric insulators due to aging [23–25]. Defects in transmission and distribution lines cause non-sinusoidal signals. J. Fourier showed that non-sinusoidal periodic waves consist of the sum of many sinusoidal waves with different amplitudes and frequencies. It is possible to separate non-sinusoidal waves into sinusoidal waves with varying amplitude frequencies with Fourier series [26].

The Fourier transform of an f(t) is as follows:

$$F(\omega) = \int_{-\infty}^{\infty} f(t) e^{-j\omega t} dt \tag{1}$$

The inverse Fourier transform of an $F(\omega)$ is as follows:

$$f(t) = \frac{1}{2\pi} \int_{-\infty}^{\infty} F(\omega) e^{j\omega t} d\omega \tag{2}$$

In Eq. (1) and (2),
$f(t)$: To be analyzed signal.
$F(\omega)$: Fourier transform of signal.
t: Time.
$e^{j\omega}$: Transform function.

These two equations are used to convert any function of the time or frequency domain $(-\infty, \infty)$ to a continuous function in the inverse domain.

During the experiment, the leakage currents flowing through the sample surface were transferred to the computer with an analog/digital converter over the ground electrode. The sampling frequency of the A/D converter used is 48 kHz. The recorded leakage current was decomposed into their harmonic components by Fourier transforms. In this step, Eq. (2) and Eq. (3) are used for decomposition into its harmonic components was calculated 3 s after evaporation of the number of drops where carbonation begins and cavitation starts falling onto the sample surface. The experiments were repeated 5 times for each condition. The signal recorded from the sample closest to the mean of the beginning drop number of

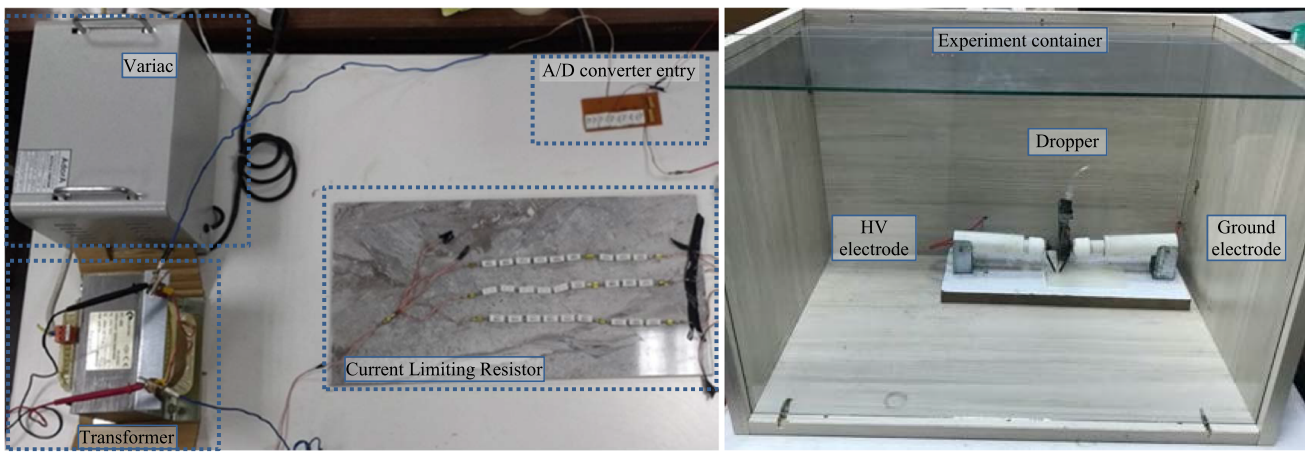

(a) **(b)**

Fig. 4 **a** Top photograph of experimental setup, **b** side photograph of the electrode arrangement

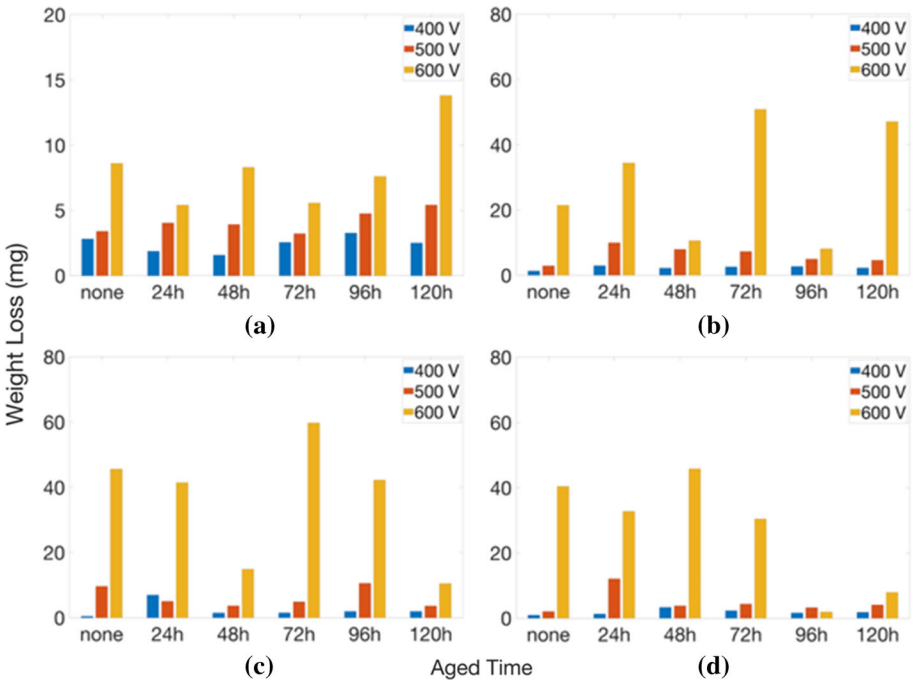

Fig. 5 Weight loss of samples in end of tests: **a** non-adding samples, **b** %1 MgO-added Samples, **c** %3 MgO-added Samples, **d** %5 MgO-added Samples

carbonization formation and cavitation beginning drop number was selected for harmonic analysis. In this study, the first 50 Hz component was obtained. Later, 150, 250, 350 and 450 Hz components were obtained. The singular harmonic distortion for n^{th} harmonic order of current was expressed by Eq. (3). Using Eq. (3) and the obtained signs, 3rd, 5th, 7th and 9th harmonic distortion values were calculated.

$$HD_n = \frac{I_{n_{max}}}{I_{1_{max}}} \tag{3}$$

In Eq. (3),
HD_n: nth harmonic distortion.
$I_{n_{max}}$: nth harmonic component.
$I_{1_{max}}$: Fundamental harmonic component.

3 Results

The weight losses occurring in the samples with testing the samples under three different voltage levels are shown in Fig. 5. The weight losses in this figure are arithmetic average of five samples results. The weight loss increased with the increase in the voltage level. The weight loss at 600 V was lower in the sample with non-adding compared to the other voltage levels (Fig. 5 (a)). In the non-adding samples, weight losses increased with the increase in the keeping time in water at all voltage levels. At 400 V and 500 V, the least weight loss is observed in the samples not kept in water with 1% MgO addition (Fig. 5b). At 600 V, the least weight loss is observed in the samples kept in water for 96 h with 1% MgO addition (Fig. 5 b). The weight loss of samples kept in water for 72 h and 120 h was approximately eight times at 600 V compared to 500 V. Approximately, the same results were observed at 400 V and 500 V levels in terms of weight loss in the samples with 3% MgO addition (Fig. 5c). The least weight loss was observed in samples that were not kept in water at 400 V, kept in water for 48 h at 500 V, kept in water for 120 h at 600 V. In the sample kept in water for 72 h, it was observed that the weight loss increased three times when the voltage level was increased from 400 to 500 V, while it increased 12 times from 500 to 600 V. The weight losses in samples with 5% MgO addition showed almost similar properties at 400 V and 500 V (Fig. 5d). In the sample kept in water for 24 h, weight loss at 500 V was four times compared to other samples. While weight loss in all samples increased with increasing 500 V to 600 V, weight loss decreased by almost 80% only in the sample kept in water for 96 h for this situation. The hydrophobic properties of the surface were deteriorated, and the harmonic values were increased in the samples that kept in water for more than 72 h. So, the material was exposed to less energy and caused less material loss with the increase in the surface conductivity.

The droplet number of the beginning of carbonization that tested the samples under three different voltage levels is shown in Fig. 6. The number of drops in this figure is arithmetic average of five samples' results. As a result of the visual examinations during the experiments, it was observed that the carbonization took place earlier with increasing the voltage level. The carbonization has taken place earlier in the samples kept in water. For non-adding samples at 400 V,

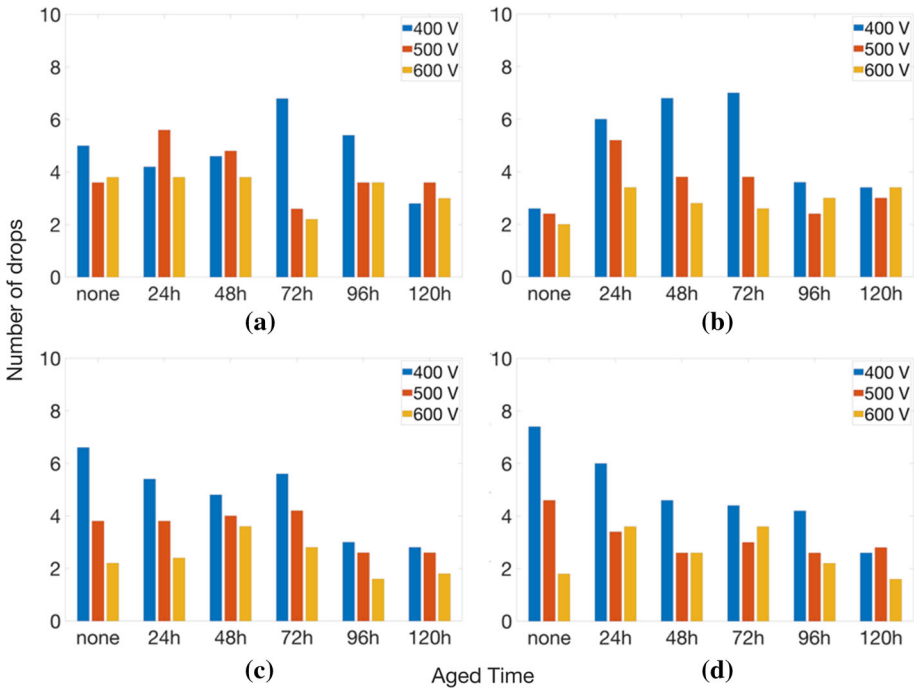

Fig. 6 Droplet number of the beginning of carbonization: **a** non-adding samples, **b** %1 MgO-added Samples, **c** %3 MgO-added Samples, **d** %5 MgO-added Samples

the longest time was observed in the sample kept in water for 72 h, while the shortest time was observed in the sample kept in water for 120 h (Fig. 6a). For non-adding samples at 500 V, the longest time was observed in the sample kept in water for 24 h, while the shortest time was observed in the sample kept in water for 72, 96 and 120 h. In experiments carried out at 600 V with non-adding samples, the beginning carbonization droplet number is approximately equal (Fig. 6a). In experiments carried out at 400 V with 1% MgO-added samples, the carbonization time decreased as the keeping time in water increased except for 24 h. In particular, there was a striking decrease in the samples kept in water for 96 and 120 h (Fig. 6b). For this adding ratio, it has been observed that keeping in water negatively affects the sample. For 1% MgO-added samples at 500 V, the longest time was observed in the sample kept in water for 24 h, while the shortest time was observed in the sample kept in water for 96 h. For 1% MgO-added samples at 600 V, the beginning of carbonization's droplet number is approximately equaled in all storing hours (Fig. 6b). In the experiments conducted with 3% MgO-added samples at 500 V and 600 V, samples kept in water and not kept in water showed approximately similar behavior (Fig. 6c). For this adding ratio, the beginning time of carbonization was significantly reduced with increased kept time in water in the experiments conducted at 400 V. Thus, it can be concluded that the tracking resistance of the samples containing 3% MgO decreased considerably with kept in water for 96 and 120 h (Fig. 6c). For 5% MgO-added samples at 400 V and 500 V, carbonization occurred earlier with the increased keep time in the water. For this adding ratio, the samples kept in water for 96 and 120 h and not kept in water showed similar behavior at 600 V (Fig. 6d). According to the number of drops where carbonization begins, it can be said that the added samples showed better performance compared to the non-adding samples.

The droplet number of the beginning of cavitation with testing the samples under three different voltage levels is shown in Fig. 7. The number of drops in this figure is arithmetic average of five samples results. The samples in which cavitation occurs latest are generally observed those with 400 V applied. The increasing voltage level was caused the cavitation to occur earlier. Comparing the non-adding samples and the added samples, cavitation occurred in a shorter time in the added samples. It can be concluded that adding is a factor that causes cavitation events earlier. In the experiments with 1% MgO-added samples, the difference between the number of drops in which cavitation occurs has decreased with the increase in the keeping time in the water. The samples kept in water for 96 h and 120 h showed similar behavior for all voltage levels. In the experiments carried out with 3% and 5% MgO-added samples under 400 V voltage, the time to form cavitation has shortened with the increase in the keeping time in the water. But this is not valid for experiments at 500 V and 600 V.

The calculated harmonic distortions of samples at 400 V are shown in Fig. 8. All the calculations belong to the droplet in which the carbonization began. From the figures, it can be seen that the 3rd harmonic component is more dominant than the other components. As the harmonic order increased, the calculated harmonic distortion decreased. In non-aged

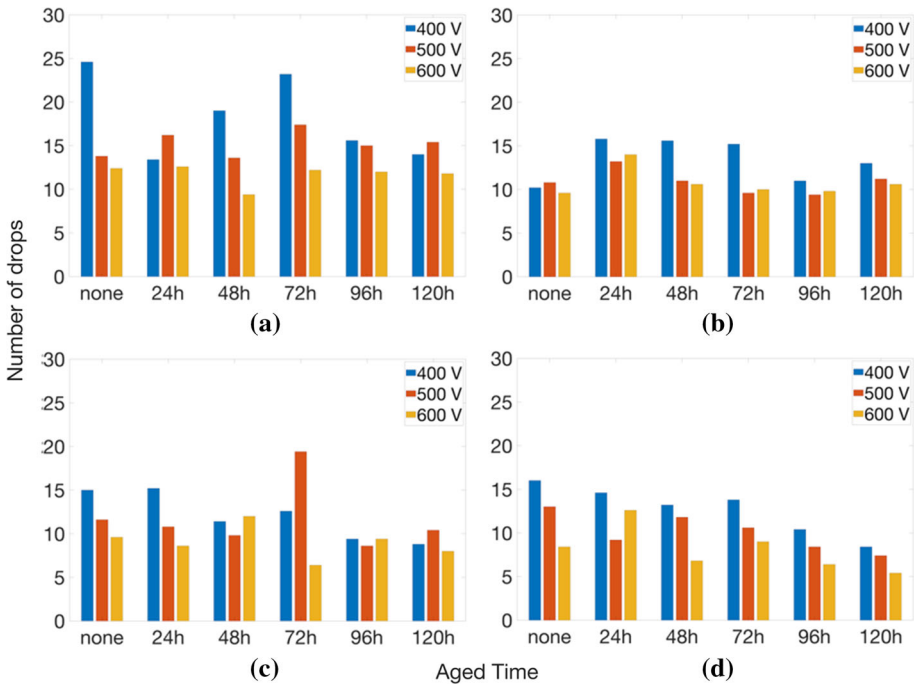

Fig. 7 Droplet number of the beginning of cavitation: **a** non-adding samples, **b** %1 MgO-added Samples, **c** %3 MgO-added Samples, **d** %5 MgO-added Samples

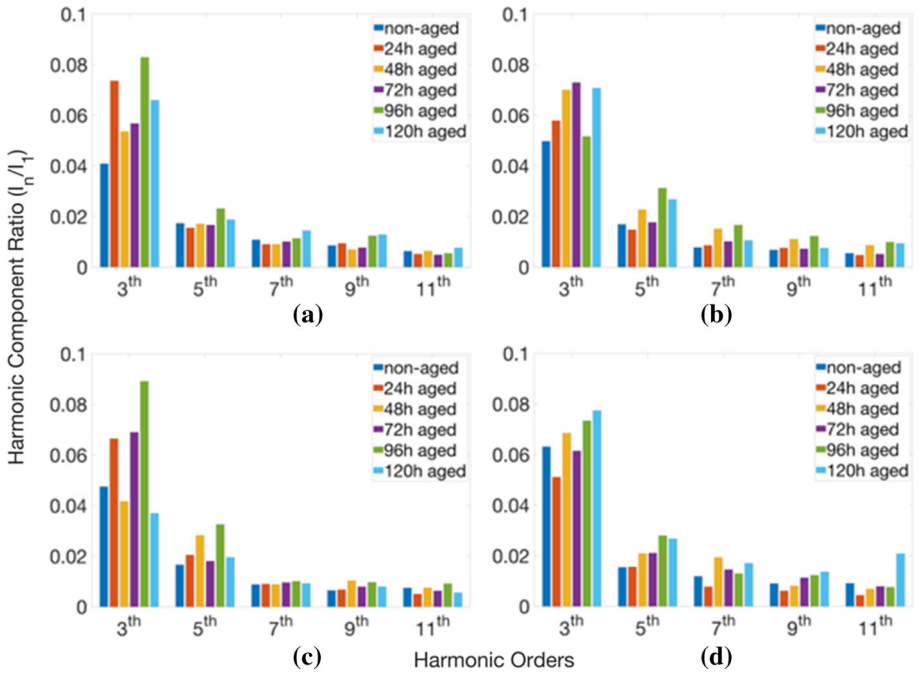

Fig. 8 Harmonic orders in the number of drops of formation of carbonization under 400 V voltage: **a** non-adding samples, **b** %1 MgO-added Samples, **c** %3 MgO-added Samples, **d** %5 MgO-added Samples

samples, the 3rd harmonic is the most dominant in the 5% MgO-added sample (Fig. 8d). In the non-aged sample in Fig. 8d, harmonic distortion of more than 5% was calculated. The negative effect of aging with water was observed at the highest in the 3rd harmonic distortion order. For all samples for the 5th harmonic order, it was observed that 96 h-aged samples were affected more negatively than the other samples. For the 11th harmonic order of the 5% MgO sample (Fig. 8d), the 120 h-aged sample was affected more negatively than the other samples at the same voltage level and harmonic order.

The calculated harmonic distortions of samples at 500 V are shown in Fig. 9. All the calculations belong to the droplet in which the carbonization began. From the figures, it can be seen that the 3rd harmonic component is more dominant than the other components. As the harmonic order increased, the

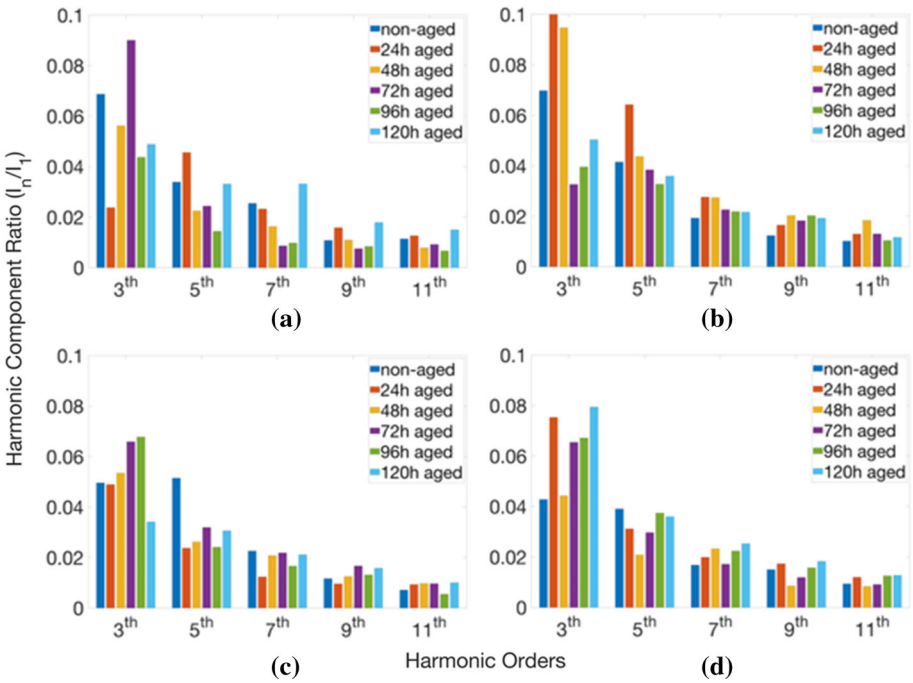

Fig. 9 Harmonic orders in the number of drops of formation of carbonization under 500 V voltage: **a** non-adding samples, **b** %1 MgO-added Samples, **c** %3 MgO-added Samples, **d** %5 MgO-added Samples

calculated harmonic distortion decreased. The harmonic distortions at 500 V were higher than the harmonic distortions at 400 V. When the voltage level increased above 500 V, the 3rd harmonic distortion increased above 5%. For the non-adding sample (Fig. 9 (a)), the least affected sample in water aging was a 24 h-aged sample for the 3rd harmonic distortion. However, the most negative case for the 5th harmonic distortion was observed in the 24 h-aged sample. For non-adding samples (Fig. 9a), the harmonic distortions of the 120 h-aged sample decreased as the harmonic level increased. For 1% MgO-added samples (Fig. 9b), more harmonic distortion was calculated for 24 h-aged and 48 h-aged samples compared to the non-aged sample for the 3rd harmonic order. 72 h-aged, 96 h-aged and 120 h-aged samples had a harmonic distortion below 5%. At the 5th harmonic order, 24 h-aged samples had almost two times higher harmonic distortion than the samples at the same level. It can be said that the 7th, 9th and 11th harmonic orders were affected similarly. For 3% MgO-added samples (Fig. 9c), the harmonic distortion increased as the water aging duration increased in the 3rd harmonic order. The most negative effect was seen for the non-aged sample for the 5th harmonic order. The samples in Fig. 9 with 3% MgO addition were the adding ratio with the lowest harmonic distortion. For 5% MgO-added samples (Fig. 9d), non-aged and 48 h-aged samples at the 3rd harmonic order had the harmonic distortion below 5%. The effect of water aging increased the harmonic distortion as the water aging duration increased by 5% adding ratio.

The calculated harmonic distortions of samples at 600 V are shown in Fig. 10. All the calculations belong to the droplet in which the carbonization began. From the figures, it can be seen that the 3rd harmonic component is more dominant than the other components according to signal of selected sample. As the harmonic order increased, the calculated harmonic distortion decreased. The highest harmonic at 600 V was calculated for 5% MgO samples. For non-adding samples (Fig. 10a), the aging water effect caused the harmonic distortion to increase three times. The lowest effect of water was observed in the 120 h-aged sample. For 1% MgO-added samples (Fig. 10b), the 3rd harmonic order was below 5% level only for 72 h-aged sample. The lowest harmonic distortion at the 5th harmonic order was calculated for the non-aged sample. As the water aging duration increased, the harmonic distortions at the 5th harmonic order increased. For 3% MgO-added samples (Fig. 10c), the 3rd harmonic order was above 5% for 72 h-aged and 96 h-aged samples. The most negative effect was seen for the 96 h-aged sample as the harmonic level increased. For 1% MgO-added samples (Fig. 10d), the 3rd harmonic order was below 5% level only for 48 h-aged sample. Other samples at the 3rd harmonic order were negatively affected by water aging.

The calculated harmonic distortions of samples at 400 V are shown in Fig. 11. All the calculations belong to the droplet in which the carbonization began. From the figures, it can be seen that the 3rd harmonic component is more dominant than the other components. As the harmonic order increased, the calculated harmonic distortion decreased. For the non-adding samples (Fig. 11a), the lowest 3rd harmonic distortion was calculated for the non-aged sample. For the 3rd harmonic order, a harmonic distortion above 5% was calculated for

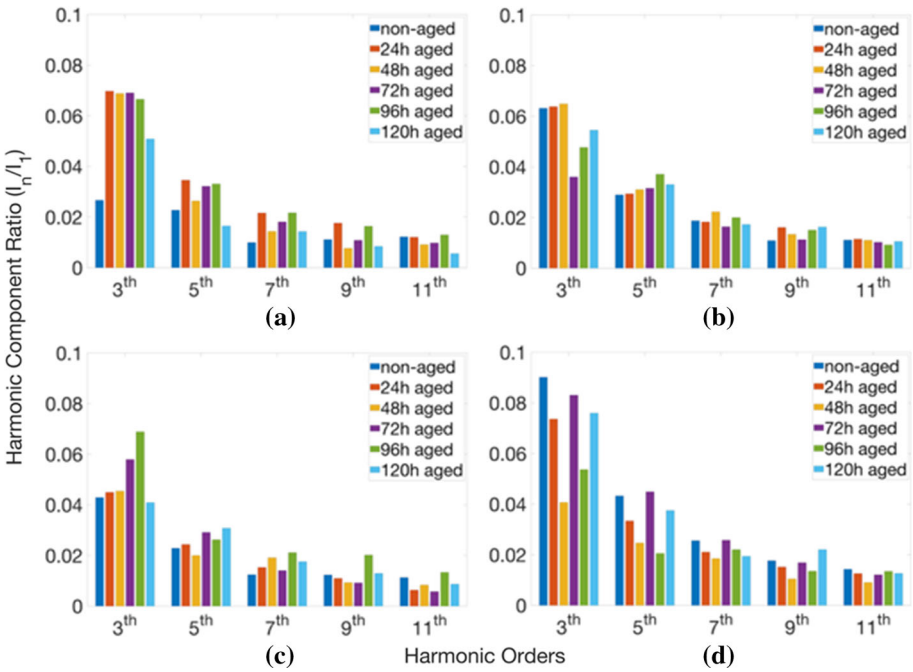

Fig. 10 Harmonic orders in the number of drops of formation of carbonization under 600 V voltage: **a** non-adding samples, **b** %1 MgO-added Samples, **c** %3 MgO-added Samples, **d** %5 MgO-added Samples

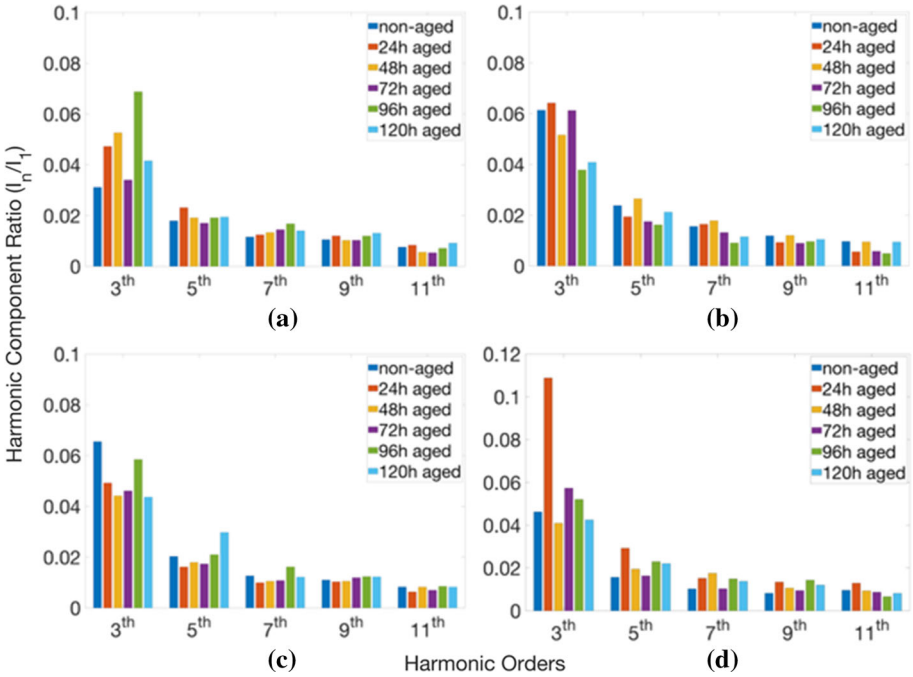

Fig. 11 Harmonic orders in the number of drops of formation of cavitation under 400 V voltage: **a** non-adding samples, **b** %1 MgO-added Samples, **c** %3 MgO-added Samples, **d** %5 MgO-added Samples

24 h-aged, 48 h-aged, 72 h-aged and 96 h-aged samples. 120 h-aged sample, which is a water-aged sample, generated the least harmonic among the samples with water aging. In samples with 1% MgO addition (Fig. 11b), when the 3rd harmonic distortion was analyzed, 96 h-aged and 120 h-aged samples had harmonic distortion below 5% harmonic distortion. At the 5th harmonic order, the 48 h-aged sample had a higher harmonic compared to other samples. In samples with 3% MgO addition (Fig. 11c), when the 3rd harmonic distortion was analyzed, non-aged and 96 h-aged samples had harmonics above 5% harmonic distortion. In the 5th harmonic distortion, the 120 h-aged sample had higher harmonic distortion compared to the samples at the same level. Samples at the 7th, 9th and 11th harmonic orders had a similar harmonic distortion. In samples with 5% MgO addition (Fig. 11d), when the 3rd harmonic distortion was analyzed,

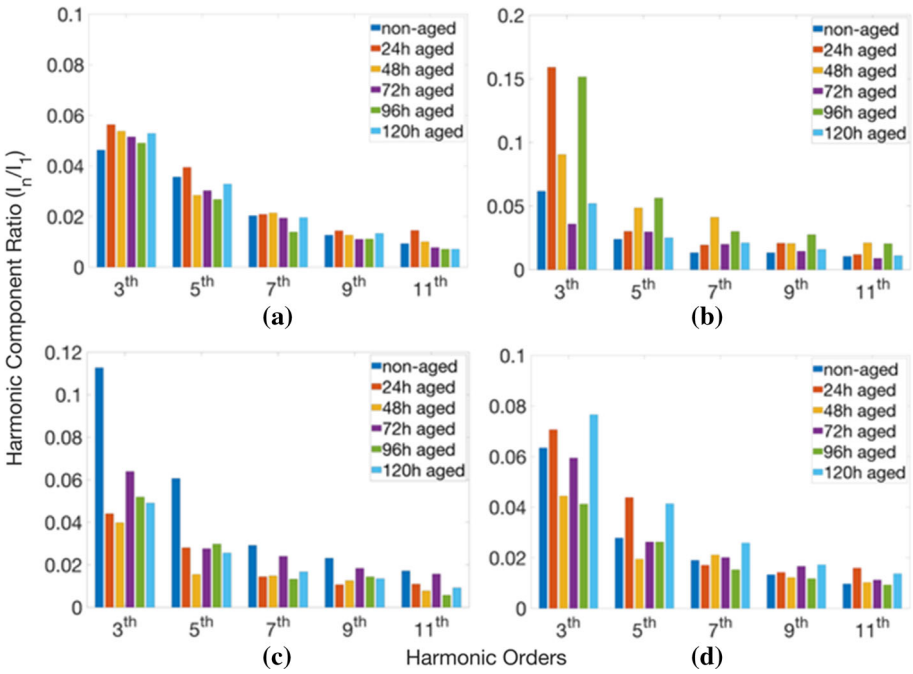

Fig. 12 Harmonic orders in the number of drops of formation of cavitation under 500 V voltage: **a** non-adding samples, **b** %1 MgO-added Samples, **c**) %3 MgO-added Samples, **d** %5 MgO-added Samples

the 24 h-aged sample had 2.5 times higher harmonic distortion than the non-aged sample. For the 5% adding ratio, the least harmonic distortion occurred in the 48 h-aged sample.

The calculated harmonic distortions of samples at 500 V are shown in Fig. 12. All the calculations belong to the droplet in which the carbonization began. From the figures, it can be seen that the 3rd harmonic component is more dominant than the other components. As the harmonic order increased, the calculated harmonic distortion decreased. For non-adding samples (Fig. 12a), it was observed that water aging increased harmonic distortion. For the 3rd harmonic order, the samples affected from the water had harmonic distortion above 5% level. As the harmonic order increased, higher harmonic distortion was calculated for the 24 h-aged sample. For 1% MgO-added samples (Fig. 12b), the only 72 h-aged sample had harmonic distortion below 5% for the 3rd harmonic distortion. As the harmonic distortion order increased, the highest harmonic distortions were observed in 48 h-aged and 96 h-aged samples. For the 3% MgO-added sample (Fig. 12c), the highest harmonic distortion was observed in the non-aged sample for the 3rd harmonic distortion. At the 3rd harmonic distortion level, 24 h-aged and 48 h-aged samples had harmonics below 5% harmonic distortion. The high harmonic distortions in the non-aged sample also occurred in other harmonic levels. The lowest harmonics were observed for the 48 h-aged sample. In samples with 5% MgO addition (Fig. 12d), 48 h-aged and 96 h-aged samples had harmonic distortion below 5% harmonic distortion for the 3rd harmonic distortion. For the 5th harmonic level, 24 h-aged and 120 h-aged samples had higher harmonic. For the 7th harmonic, the 120 h-aged sample had a higher harmonic.

The calculated harmonic distortions of samples at 600 V are shown in Fig. 13. All the calculations belong to the droplet in which the carbonization began. From the figures, it can be seen that the 3rd harmonic component is more dominant than the other components. As the harmonic order increased, the calculated harmonic distortion decreased. The harmonic distortions observed in the material were higher at 600 V compared to samples with 400 V and 500 V. In non-adding samples (Fig. 13a), calculated harmonics for all samples were above 5% for the 3rd harmonic order. Similar results, as the harmonic level recorded more than 5%, were obtained as the harmonic order increased. The 72 h-aged sample was the sample with the lowest harmonic. For samples with 1% MgO addition (Fig. 13b), there was harmonic distortion below 5% only for the 120 h-aged sample at the 3rd harmonic order. It was observed that the 24 h-aged sample harmonic distortion decreased as the harmonic level increased. In 3% MgO-added samples (Fig. 13c), a harmonic distortion below 5% was observed for the non-aged sample at the 3rd harmonic order. While high harmonics were observed in samples aged with water, the highest harmonic was observed in the 72 h-aged sample. While the lowest harmonics were observed in the non-aged sample as the harmonic order increased, the lowest harmonics were observed in the 24 h-aged sample. For 72 h-aged and 96 h-aged samples, the highest harmonic distortion was in the 7th and 9th harmonic order. For 5% MgO-added samples (Fig. 13d), high harmonic distortions were observed in all samples at the 3rd harmonic order. The highest harmonic was calculated in the non-aged sample. The highest harmonics for the 3rd, 5th and 9th harmonics were calculated

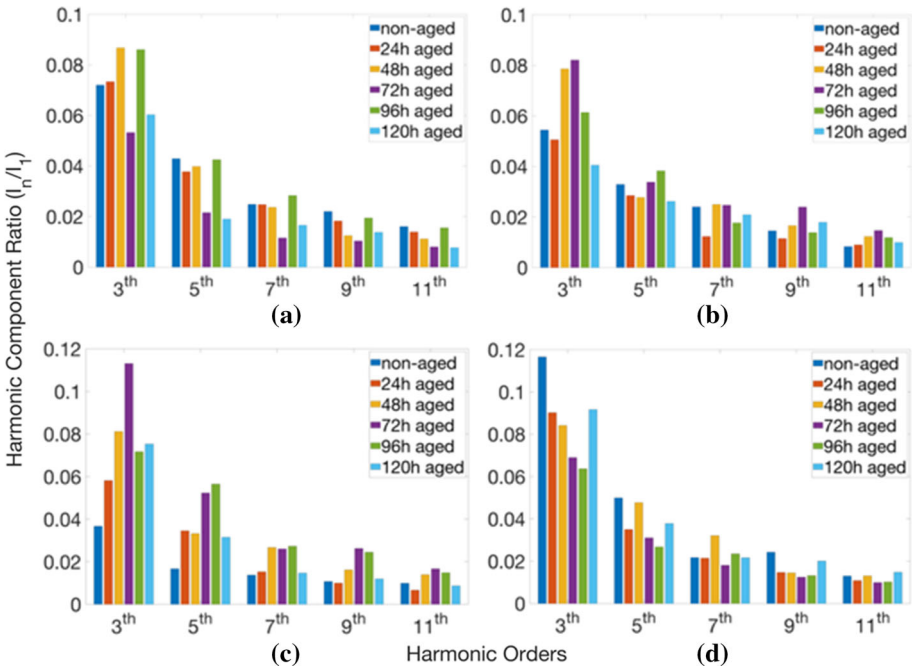

Fig. 13 Harmonic orders in the number of drops of formation of cavitation under 600 V voltage: **a** non-adding samples, **b** %1 MgO-added Samples, **c** %3 MgO-added Samples, **d** %5 MgO-added Samples

for non-aged samples. The highest harmonic distortion at the 7th harmonic order was calculated for 48 h-aged sample.

4 Conclusions

In this study, the tracking performance of epoxy/MgO samples has been evaluated under the effect of kept in water for different times, which is a coercive environmental parameter. Non-adding and MgO-added samples were tested according to IEC 60,112. The effect of adding MgO and keeping in the water on tracking resistance of samples was evaluated by experimental data and analysis of leakage current. The results obtained as a result of the studies are as follows:

- The tracking resistance of the samples containing 3% MgO was decreased significantly with kept in water for 96 and 120 h under 400 V.
- For epoxy insulation materials, it has been demonstrated by CTI experiments that the requirement to apply a minimum of 5% nanosized MgO addition will be more suitable in terms of electrical efficiency. As a result of the experiments, it was seen that 1% MgO and 3% MgO additions were not sufficient for the epoxy insulation materials.
- It is observed that samples kept in the water for 96 h are more adversely affected than other samples at 400 V in all samples for the 5th harmonic order.
- For 5% adding ratio, harmonic distortion levels have increased as the keeping time in water increased at 500 V.
- The highest harmonic at 600 V was calculated for 5% MgO samples. 5th harmonic distortion has increased as the keeping time in water increased at 600 V.
- It has been observed that keeping in the water more increased harmonic distortion in non-adding samples. The MgO-added samples were less affected by keeping in water.

It has been observed that the addition of MgO improves the tracking resistance of the epoxy samples. These results are in line with previous studies. But it was found that their insulation performance decreased in the opposite way after exposure to pure water. In this way, it is necessary to add some hydrophobic compounds in order to improve the insulation performance of MgO-added epoxy resin in the external environment with these experimental studies. Besides, the insulation materials can be supplemented with extra protection in such dense liquid environments.

Acknowledgement This study was supported by the Scientific Research Projects Coordination Unit of Istanbul University-Cerrahpasa (Project No. FYL 2019 -34046).

References

1. Du BX (2001) Discharge energy and dc tracking resistance of organic insulating materials. IEEE Trans Dielectr Electr Insul 8(6):897–901
2. Du BX, Zhang JW, Liu Y (2012) Effect of concentration on tracking failure of epoxy/TiO 2 nanocomposites under dc voltage. IEEE Trans Dielectr Electr Insul 19(5):1750–1759

3. Kozako M, Fuse N, Ohki Y, Okamoto T, Tanaka T (2004) Surface degradation of polyamide nanocomposites caused by partial discharges using IEC ž b/ electrodes. IEEE Trans Dielectr Electr Insulat 11(5):833–839
4. Yılmaz AE, İspirli MM (2018) Recurrence plot analysis of unsatured polyester samples subjected to contamination. Electrica 18(1):13–18
5. Tanaka Toshikatsu, Montanari GC, Mulhaupt R (2004) Polymer nanocomposites as dielectrics and electrical insulation-perspectives for processing technologies, material characterization and future applications. IEEE Trans Dielectr Electr Insulat 11(5):763–784
6. Wang Z, Wu K, Li J (2017) "Study of surface tracking on epoxy/MgO nanocompisite". In: 1st International Conferance on Electrical Materials and Power Equipment. pp 336–339
7. GuoY, Du BX, Xiao M, Li Y, Du H (2014) "Effects of Adding Rate on DC Tracking Failure of Epoxy/MgO Nano-composites Under Contamined Conditions". In: Conference Proceedings of ISEIM, pp. 273–276
8. Du BX, Guo YG, Liu Y (2014) Effect of adding nanofiller on DC tracking failure of epoxy/MgO nanocomposites under contaminated conditions. IEEE Trans Dielectr Electr Insulat 21(5):2146–2155
9. Wu K, Wang Z (2018) Surface treeing and sengmented worm model of tracking behaviour in MgO/Epoxy nanocomposites. IEEE Trans Dielectr Electr Insulat 25(6):2067–2075
10. Du BX, Zhang JW, Liu Youg (2011) Effect of concentration on tracking failure of epoxy/TiO2 nanocomposites under dc voltage. IEEE Trans Dielectr Electr Insulat 19(5):1750–1759
11. Lee SB, Lee HJ, Hong IK (2012) Diluent filler particle size effect for thermal stability of epoxy type resin. J Industr Eng Chem 18:635–641
12. Du BX, Zhang JW, Gu L, Liu HJ (2010) Application of nonlinear methods in tracking failure test of epoxy/SiO2 nanocomposites. Int Conf Solid Dielectr 17(2):548–554
13. Sarathi R, Rajesh Kumar P, Sahu RK (2007) Analysis of surface degradation of epoxy nanocomposite due to tracking under AC and DC voltages. Polymer Degradit Stability 92:560–568
14. H. Nguyen, A. Y. Mizra, W. Chen, J. Ronzello, S. Nasreen, J. Chapman, A. Bazzi, Y. Cao, (2018) "Discharge resistant epoxy/clay nanocomposite for high torque density electrical propulsion". In: IEEE conference of electrical insulation and dielectric phenomena, pp.171–174
15. Wu X, Wang Y, Xie L, Yu J, Liu F, Jing P (2013) Thermal and electrical properties of epoxy composites at high alumina loadings and various temperatures. Iran Polymer Petrochem Instit 22:61–73
16. Al-Bayer R, Zihlif A, Lahlouh B, Elimat Z, Ragosta G (2013) AC electrical and optical characterization of epoxy-Al2O3 composites. J Mater Sci: Mater Electron 24:2866–2872
17. B. X. Du, J. W. Zhang, L. Gu, M. J. Tu, Z. Q (2010) Wang and D. M. Du "Application of Nonlinear Methods in Tracking Failure Test of Silicone Rubber Nanocomposite", Annual Report Conference on Electrical Inslulation and Dielectric Phenomena
18. Z. Y. Li, Y. Gao, M. H. Wang, N. Zhao, B. X. Du, (2018) "Surface Charge Accumulation of Epoxy/Al2O3 Nanocomposites Under Magnetic Field", IEEE
19. Kumagai S, Xinsheng W, Yoshimura N (2000) Thermal aging, water absorption, and their multiple effects on tracking resistance of epoxy for outdoor use. Denki Gakkai Ronbunshi 118-A(11):1255–1263
20. Ispirli MM, Yilmaz AE, Kalenderli Ö (2018) Investigation of tracking phenomenon in cable joints as 3D with finite element method. Electr Eng 100(4):2193–2203
21. ASTM D5288–14 (2014) Standard Test Method for Determining Tracking Index of Electrical Insulating Materials Using Various Electrode Materials (Excluding Platinum), ASTM International, West Conshohocken, PA
22. IEC Publication 60112 (2009) Method for the Determination of the Proof and the Comparative Tracking Indices of Solid Insulating Materials. 4th eds. Geneva, IEC: Switzerland
23. Ahmadi-Joneidi I, Majzoobi A, Shayegani-Akmal AA, Mohseni H, Jadidian J (2013) Aging evaluation of silicone rubber insulators using leakage current and flashover voltage analysis. IEEE Trans Dielectr Electr Insul 20(1):212–220
24. El-Hag AH, Jayaram SH, Cherney EA (2003) Fundamental and low frequency harmonic components of leakage current as a diagnostic tool to study aging of RTV and HTV silicone rubber in salt-fog. IEEE Trans Dielectr Electr Insul 10(1):128–136
25. Ispirli MM, Yilmaz AE (2018) An investigation on characteristics of tracking failure in epoxy resin with harmonic and fractal dimension analysis. Turk J Electr Eng Comput Sci 26(1):245–256
26. Brigham EO, Morrow RE (1967) The fast Fourier transform. IEEE Spectr 4(12):63–70